Gene expression profiling of giant cell tumor of bone reveals downregulation of extracellular matrix components decorin and lumican associated with lung metastasis

ARTICLE *in* ARCHIV FÜR PATHOLOGISCHE ANATOMIE UND PHYSIOLOGIE UND FÜR KLINISCHE MEDICIN · OCTOBER 2014

Impact Factor: 2.65 · DOI: 10.1007/s00428-014-1666-7 · Source: PubMed

13 AUTHORS, INCLUDING:

Eberhard Korsching
University of Münster
74 PUBLICATIONS **1,104** CITATIONS
SEE PROFILE

Piero Picci
Istituto Ortopedico Rizzoli
517 PUBLICATIONS **13,290** CITATIONS
SEE PROFILE

Pancras C W Hogendoorn
Leiden University Medical Centre
472 PUBLICATIONS **15,020** CITATIONS
SEE PROFILE

Ramses Forsyth
University Hospital Brussels
55 PUBLICATIONS **999** CITATIONS
SEE PROFILE

Virchows Arch
DOI 10.1007/s00428-014-1666-7

ORIGINAL ARTICLE

Gene expression profiling of giant cell tumor of bone reveals downregulation of extracellular matrix components decorin and lumican associated with lung metastasis

M. Lieveld · E. Bodson · G. De Boeck · B. Nouman · A. M. Cleton-Jansen · E. Korsching · M. S. Benassi · P. Picci · G. Sys · B. Poffyn · N. A. Athanasou · P. C. W. Hogendoorn · R. G. Forsyth

Received: 1 May 2014 / Revised: 21 August 2014 / Accepted: 3 October 2014

Abstract Giant cell tumor of bone (GCTB) displays worrisome clinical features such as local recurrence and occasionally metastatic disease which are unpredictable by morphology. Additional routinely usable biomarkers do not exist. Gene expression profiles of six clinically defined groups of GCTB and one group of aneurysmal bone cyst (ABC) were determined by microarray (n=33). The most promising differentially expressed genes were validated by Q-PCR as potential biomarkers in a larger patient group (n=41). Corresponding protein expression was confirmed by immunohistochemistry. Unsupervised hierarchical clustering reveals a metastatic GCTB cluster, a heterogeneous, non-metastatic GCTB cluster, and a primary ABC cluster. Balanced score testing indicates that lumican (LUM) and decorin (DCN) are the most promising biomarkers as they have lower level of expression in the metastatic group. Expression of dermatopontin (DPT) was significantly lower in recurrent tumors. Validation of the results was performed by paired and unpaired t test in primary GCTB and corresponding metastases, which proved that the differential expression of LUM and DCN is tumor specific rather than location specific. Our findings show that several genes related to extracellular matrix integrity (LUM, DCN,

M. Lieveld (✉) · E. Bodson · G. De Boeck · B. Nouman · R. G. Forsyth
N. Goormaghtigh Institute of Pathology, Ghent, Belgium
e-mail: marusyalieveld@hotmail.com

E. Bodson
e-mail: erikbodsonmd@gmail.com

G. De Boeck
e-mail: deboeckgitte@yahoo.com

B. Nouman
e-mail: nouman.bouchra@yahoo.com

R. G. Forsyth
e-mail: r@forsyth.be

A. M. Cleton-Jansen · P. C. W. Hogendoorn
Department of Pathology, Leiden University Medical Center, Leiden, The Netherlands

A. M. Cleton-Jansen
e-mail: A.M.Cleton-Jansen@lumc.nl

P. C. W. Hogendoorn
e-mail: P.C.W.Hogendoorn@lumc.nl

E. Korsching
Institute of Bioinformatics, University of Muenster, Muenster, Germany
e-mail: korschi@uni-muenster.de

M. S. Benassi · P. Picci
Laboratorio di Ricerca Oncologica, Istituto Ortopedico Rizzoli, Bologna, Italy

M. S. Benassi
e-mail: mariaserena.benassi@ior.it

P. Picci
e-mail: piero.picci@ior.it

G. Sys · B. Poffyn
Department of Orthopaedic Surgery, Ghent University Hospital, Ghent, Belgium

G. Sys
e-mail: gwen.sys@UGent.be

B. Poffyn
e-mail: bart.poffyn@uzgent.be

N. A. Athanasou
Department of Pathology, Nuffield Department of Orthopaedic Surgery, Nuffield Orthopaedic Centre, Oxford, UK

e-mail: Nick.Athanasou@ouh.nhs.uk

M. Lieveld
ICRH, Ghent University, De Pintelaan 185 UZP114, 9000 Ghent, Belgium

Published online: 11 October 2014

and DPT) are differentially expressed and may serve as biomarkers for metastatic and recurrent GCTB.

Keywords Giant cell tumor of bone · Decorin · Osteoclastogenesis · Gene expression profiling · Extracellular matrix

Abbreviations

GCTB	Giant cell tumor of bone
ABC	Primary aneurysmatic bone cyst
ECM	Extracellular matrix
cRNA	Copy ribonucleic acid
DCN	Decorin
LUM	Lumican, DPT, dermatopontin
EPYC	Epiphycan
ZNF14	Zinc finger protein-14
CLEC2D	C-type lectin domain family 2-member D
RPL23	Ribosomal protein L23
FRZB	Frizzled-related protein
C2orf40	Chromosome 2 open reading frame 40
FGFBP2	Fibroblast growth factor binding protein 2
CPXM2	Carboxypeptidase X-M14 family-member 2
PEG3	Paternally expressed 3
TGF-β	Transforming growth factor beta
NRQ	Normalized relative quantity
DAB	Diaminobenzidine
M-CSF	Macrophage colony-stimulating factor
RANKL	Receptor activator of nuclear factor kappa-B ligand
VEGF	Vascular endothelial growth factor
HGF	Hepatocyte growth factor/scatter factor
HIF-1α	Hypoxia-inducible factor 1-alpha
TKR	Tyrosine kinase receptor
TNF-α	Tumor necrosis factor α
IL-6	Interleukin-6
LIGHT	Tumor necrosis factor superfamily, member 14
PIGF	Placental growth factor
FLT-3	Fms-like tyrosine kinase 3
HGF	Hepatocyte growth factor
MET	HGF receptor
MMP-9	Matrix metalloprotein 9

Introduction

Giant cell tumor of bone (GCTB) is an osteolytic bone tumor which occurs most commonly in patients who have reached skeletal maturity. It usually arises in the epiphysis of long bones and consists of a population of mostly inconspicuous spindle-shaped fibroblast-like stromal cells and more conspicuous populations of monocytoid cells and osteoclast-like giant cells. The spindle cell component seems to be responsible for the attraction of blood monocytes, immigration, and differentiation of osteoclasts and osteoclast activity [1]. In cell cultures, osteoclasts are lost after a few generations [2].

GCTB shows variable behavior in terms of tumor growth and metastatic potential. In most cases, it behaves as a benign, gradually enlarging osteolytic bone tumor but in some cases it shows rapid growth and local aggressiveness: Rarely, metastatic lung nodules of GCTB can develop and malignant change in GCTB can also occur. Osteolytic and locally aggressive characteristics of GCTB can be explained by its cathepsin biology and high degree of RANKL expression which is associated with increased osteoclast formation and activity [3–5]. Intravascular plugs of GCTB can be found at the periphery of the tumor, but a clear mechanism for metastatic disease has not yet been elucidated [6, 7].

The treatment of GCTB largely depends on its extension. Most cases are treated by curettage but local recurrence is common and extensive 'en bloc' resection may be the only curable option [8–10]. Anticipating clinical behavior of GCTB is important in planning appropriate therapy and avoiding repetitive surgical interventions [10–12].

To date, no histological, clinical or radiographic characteristics have clearly been shown to predict the behavior of GCTB in terms of outcome [6, 13–15]. In contrast, gene expression profiling has been proven to be of value in identifying specific genes that predict tumor behavior. The aim of this study was to obtain greater insight into the biological behavior of GCTB through identification of gene expression profiles that might act as biomarkers, capable of distinguishing subgroups of GCTB with distinctly different clinical behaviors. In addition, we set out to determine whether the biomarkers we identified are site specific (expressed preferentially in lung metastasis but not in the primary tumor) or tumor specific (expressed in metastases as well as their primary tumors but not in non-metastasizing tumors).

Materials and methods

Patient and tissue sample selection

Cases were selected from the archives of the departments of Pathology of Leiden University Medical Center (The Netherlands) (n=23), the N. Goormaghtigh Institute of Pathology of the Ghent University Hospital (Belgium) (n=6), and the Rizolli Institute Bologna (Italy) (n=4). A total of 24 patients with GCTB, five patients with primary ABC and four patients with GCTB lung metastases were included for microarray analysis. The heterogenous group of 24 GCTBs was subdivided into five subgroups: conventional GCTB (control group; GCTB-0), GCTB with regressive changes (fibrosis, hemorrhages, and foam cell aggregates; GCTB-R), a high recurrence group (at least third recurrence of GCTB at

the same location; GCTB-3R), GCTB located in the distal radius (GCTB-A), and GCTB with secondary ABC (GCTB-ABC). None of these patients were treated with denosumab before sampling. The ABC group was used as a second control group, representing a benign giant cell-rich bone tumor distinct from GCTB. There were no solid variants included in the ABC group. A snap frozen section of the whole tumor sample was made, hematoxylin and eosin stained and examined independently by two pathologists (PCW and RGF) in order to confirm subsequent diagnoses and to exclude excessive contamination by bone or other non-tumoral tissue. Finally, 20 sections (20 μm) of each sample were cut and stored at −80 °C until use for gene expression analysis. For quantitative polymerase chain reaction (Q-PCR), an additional eight patients (N. Goormaghtigh Institute of Pathology of the Ghent University Hospital (Belgium)) were included: three in the control group, two in the high recurrence group, two cases of GCTB with secondary ABC, and one patient with GCTB located in the distal radius. Biomarkers for lung metastases were evaluated in an independent set of 11 samples (the Rizolli Institute Bologna (Italy)): six cases of GCTB-M and their corresponding primary tumor (GCTB-P); for one lung metastasis no primary bone tumor was available.

Microarray analysis

Illumina's Human-6 v2 Expression BeadChips (Illumina®, Son, The Netherlands) were used. This genome-wide expression platform simultaneously profiles six sample and more than 48,000 transcript probes per sample, on a single microarray and 30 to 40 replicates of each bead are used, generating very reliable data. The expression beads contain full-length 50-mer probes of well characterized genes, gene candidates, and splice variants. These gene-specific probes carry 100,000 copies of the probe attached to the bead surface, binding the biotin labeled copy RNA (cRNA) in the sample. The biotin labeled cRNA is generated from total RNA, isolated from each of the tumor samples. After hybridization to the Illumina's Human-6 Expression BeadChip Arrays, the generated data were analyzed applying the Illumina's BeadStudio Software.

RNA extraction, cRNA synthesis, and hybridization of microarray targets

Total RNA was isolated from GCTB tissue, sectioned into 20 μm sections using a cryostat, with Trizol® (Invitrogen Life Technologies, Carlsbad, CA) and purified using the RNeasy-mini kit (Qiagen, Hilden, Germany), according to the user manuals. The quantity of RNA was measured with the NanoDrop ND-100 Spectrophotometer (Nanodrop® Technologies Inc., Wilmington, DE), and the quality was verified on the Agilent 2100 Bioanalyzer (Agilent Technologies, Palo Alto, CA). Of the quality-checked RNA, 200 ng was transposed in biotin labeled amplified cRNA, using the Illumina® TotalPrep RNA Amplification Kit (Ambrion, Inc., Austin, TX). In this way, multiple copies of biotin labeled cRNA were synthesized and, after purification, hybridized to the Illumina's human −6 V2 Human-6 v2 Expression BeadChip Arrays. The arrays were washed, blocked, and stained with streptavidin-Cy3 solution. The fluorescent assay signal, generated on each array, was captured and quantified using the Illumina BeadArray Reader. Output files were exported to the Illumina's Beadstudio Software for analysis. Bead signals were computed with weighted averages of pixel intensities and local background was subtracted.

Statistical analysis

An unsupervised hierarchical cluster analysis, ClustalW, using correlation-based average linkage clustering was applied to assess the relative similarities or dissimilarities in the global gene expression patterns. The gene expression profiles of the different groups were compared to each other using the balanced test method, which can identify the most significant and biologically relevant markers and rank these according to their biological relevance [16]. As a different approach, this methodology first test the null hypothesis followed by a second test with an alternative hypothesis of interest (in our case, twofold change in messenger RNA [mRNA] level). The results of both tests are depicted in a global R value, being the ration of p values of the alternative over the null hypothesis. In this method, the null hypothesis is rejected, if $R>1$. The genes with the highest R values in each group are considered most relevant.

Validation by quantitative polymerase chain reaction

RNA extraction

As a complement to the samples used for microarray, eight additional samples (three for GCTB-0, two for GCTB-3R, one for GCTB-A, and two GCTB-ABC) were included for Q-PCR (Table 1). Potential biomarkers for GCTB with lung metastases were evaluated in a supplementary group of 11 cases (Table 1). For each sample, 25 mg of tissue was disrupted and the lysate was homogenized with a rotar-stator homogenizer. Total RNA was extracted with the RNeasy Mini Kit (Qiagen, Venlo, The Netherlands) following the manufacturer's instructions. This was followed by a DNase treatment using RQ1 RNase-Free DNase (Promega, Leiden, The Netherlands), ensuring that only RNA is present in the sample. After the DNase treatment, first-strand cDNA was synthesized using the iScript cDNA synthesis kit (Biorad Laboratories Ltd. Hertfordshire, UK) according to the manufacturer's directions. The cDNA concentrations in the samples were

Table 1 Clinicopathological data of 36 GCTB and five primary ABC tumor samples, subdivided into seven groups according to clinical and histological data

Patient ID	Age (years)	Sex	Localisation	Diagnosis
1	22	F	Right distal femur	GCTB-0
2	48	M	Left distal femur	GCTB-0
3	33	M	Right distal femur	GCTB-0
4	31	M	Right distal femur	GCTB-0
5	25	F	Knee	GCTB-0
6	33	M	Knee	GCTB-0
7	25	M	Knee	GCTB-0
8	32	F	Sacrum	GCTB-0
9	51	M	Sacrum	GCTB-0
10	45	F	Left distal femur	GCTB-R
11	29	M	Right distal femur	GCTB-R
12	25	M	Right distal femur	GCTB-R
13	45	F	Left distal femur	GCTB-R
14	54	M	Left distal femur	GCTB-R
15	40	F	Right distal radius	GCTB-3R
16	42	F	Right distal femur	GCTB-3R
17	22	M	Right proximal tibia	GCTB-3R
18	38	F	Left proximal tibia	GCTB-3R
19	54	M	Right distal radius	GCTB-3R
20	25	F	Right distal radius	GCTB-A
21	59	M	Left distal radius	GCTB-A
22	25	M	Left distal radius	GCTB-A
23	40	M	Left distal radius	GCTB-A
24	22	M	Right distal radius	GCTB-A
25	22	F	Right distal radius	GCTB-A
26	34	M	Left distal radius	GCTB-A
27	18	M	Left proximal tibia	GCTB-ABC
28	27	F	Left proximal tibia	GCTB-ABC
29	21	F	Right distal radius	GCTB-ABC
30	24	F	Right distal tibia	GCTB-ABC
31	22	M	Left proximal tibia	GCTB-ABC
32	30	F	Right distal radius	GCTB-ABC
33	45	F	Lung	GCTB-M
34	51	M	Lung	GCTB-M
35	39	M	Lung	GCTB-M
36	56	F	Lung	GCTB-M
42	41	M	Lung	GCTB-M
43	32	F	Lung	GCTB-M
44	25	M	Lung	GCTB-M
45	58	F	Lung	GCTB-M
46	29	M	Lung	GCTB-M
47	23	M	Lung	GCTB-M
48 (primary tumor of 42)	41	M	Left distal femur	GCTB-P
49 (primary tumor of 43)	32	F	Right distal femur	GCTB-P
50 (primary tumor of 44)	25	M	Right distal femur	GCTB-P
51 (primary tumor of 45)	58	F	Knee	GCTB-P
52 (primary tumor of 46)	29	M	Knee	GCTB-P
37	23	M	Left fibula	ABC
38	17	M	Left pedicle L4	ABC
39	12	F	Right fibula	ABC
40	26	F	Left tibia	ABC
41	15	M	Right femur	ABC

GCTB-0 samples of histologically low-grade and homogeneous tumors without any evidence of associated lesions. *GCTB-R* tumor samples showing regressive changes. *GCTB-3R* samples of a third recurrence of GCTB at the same location. *GCTB-A* samples of GCTB located in the distal radius. This location is frequently associated with a more aggressive clinical behavior. *GCTB-ABC* samples of primary GCTB with associated secondary ABC. *GCTB-M* samples of a lung metastatic nodule of GCTB. *ABC* samples of primary ABC. *GCTB-P* primary tumor of metastatic GCTB

measured by the NanoDrop ND-100 Spectrophotometer (Nanodrop Technologies Inc., Wilmington, DE). Before applying Q-PCR, cDNA was diluted up to a concentration of 20 ng/μl.

Selection of reference genes

The most stable and optimal housekeeping genes for the 41 samples were identified, with the geNorm Housekeeping Gene Selection Kit (Primerdesign, Southampton, Hants), according to its instructions.

Primer design

Specific expression primers were designed using Primer-Blast, Oligo 7, and mFold. The selected primers were synthesized by Integraded DNA Technologies (Leuven, Belgium). Primer sequences are available on request.

Q-PCR

Q-PCR was performed using the LightCycler® 480 (Roche Diagnostics, Vilvoorde, Belgium). All tests were run in duplicate and two non-template controls were included. The reaction volume in each well contained 9.6 μl Sybr Green mix (Roche Diagnostics), 0.7 μl forward primer (5 μM), 0.7 μl reverse primer (5 μM), 4 μl H_2O (Roche Diagnostics), and 2 μl cDNA (20 ng/μl). The amplification procedure was performed under the following conditions: preincubation at

95 °C for 10 min, 50 cycles of template denaturation at 95 °C for 10 s, together with 14 s of primer annealing at gene-specific temperature, and elongation at 72 °C for 12 s. To verify the specificity of the Q-PCR, a melting curve was generated at the end of each reaction, by elevating the temperature from 65 to 95 °C.

Analysis of the Q-PCR results

The raw Q-PCR data were processed and analyzed using qBase^{plus} (Biogazelle) identifying first the reference genes followed by obtaining normalized relative quantity (NRQ) for every test. For each NRQ, a standard deviation was calculated.

Statistical analysis was accomplished with the help of SPSS 17.0 software. To identify a correlation between most promising expressed genes and the defined subgroups, *t* testing was applied.

Immunohistochemistry

Immunohistochemistry was performed using independent subsets of formalin-fixed paraffin-embedded (FFPE) tumor samples. This set of samples consisted of ten cases of GCTB associated with regressive changes, five cases of primary and recurrent GCTB, three lung metastatic nodules, and five cases of GCTB associated with secondary ABC. From each sample, a 4 μm paraffin-embedded slide was cut, mounted on an electrically charged superfrost plus slide (Menzel-Gläser, Braunschweig), rehydrated, and submitted to antigen retrieval in EDTA (pH 8.0) or citrate (pH 6.0). After quenching, the sections were stained with antibodies (Abcam, UK) against proteins of interest in a dilution of 1:100 for 1 h at room temperature. Afterwards, the sections were incubated with biotinylated secondary antibody and subsequently with the streptavidin-HRP (DAKO, Heverlee, Belgium), both for 30 min at room temperature. Finally, the sections were incubated in peroxidase DAB (Diaminobenzidine) (DAKO) solution and counterstained with hematoxylin.

Results

Unsupervised hierarchical clustering

ClustalW revealed three major clusters: a metastatic cluster, a primary ABC cluster, and a large heterogeneous GCTB cluster. In the primary ABC cluster, a subcluster containing part of the GCTB control cases was present.

Microarray data

An overview of the biologically most relevant markers, identified with the balanced test method is displayed in Table 2. A comparison of metastatic with non-metastatic cases in this study identified 11 genes which showed significantly lower expression in the metastatic group. Of these 11 genes, decorin (DCN) and lumican (LUM) appeared to be the most differentially expressed genes; LUM showed 30 times less expression (p value=3E-10), and DCN was 26 (p value=4E-8) times less expressed (Fig. 1).

Regarding GCTB recurrence, four genes showed a significant differential expression in the high recurrence group. This was most prominent for dermatopontin (DPT) and zinc finger protein-14 (ZNF14); DPT exhibited lower expression whereas ZNF14 showed higher expression in the high recurrence group.

The search for potential biomarkers that might reflect regressive changes in GCTB identified epiphycan (EPYC), which was found to have a higher expression in this group. C-type lectin domain family 2-member D (CLEC2D) and ribosomal protein L23 (RPL23) showed significantly lower expression in GCTBs exhibiting regressive changes. In GCTBs with secondary ABC, a significant increase in gene expression of frizzled-related protein (FRZB), chromosome 2 open reading frame 40 (C2orf40), fibroblast growth factor binding protein 2 (FGFBP2), and carboxypeptidase X-M14 family-member 2 (CPXM2) were observed.

Gene selection and validation by Q-PCR

As noted in the above methods, 23 genes were selected for further analysis (Table 2). Q-PCR confirmed a lower expression of DCN and LUM at mRNA level in the metastatic cases (Fig. 2). From the microarray data, five genes were extracted that showed prominent differential gene expression in the relapsed cases. Differential expression was verified for two of the genes: ZNF14 displayed higher expression whereas DPT exhibited lower expression in the recurrent cases group compared to the other GCTB samples. Based on the microarray data, regressive changes in GCTB are associated with higher expression of EPYC and lower expression of CLEC2D and RPL23. Q-PCR supported differential expression of all of these three genes, however only for EPYC a significant differential expression (p=0.004) could be verified. In the GCTB group with secondary ABC, Q-PCR confirmed a significant increase in expression of FRZB.

Location specific versus tumor specific

In order to validate our findings, we investigated whether the lower expression of LUM and DCN is location specific or tumor specific. We first compared the gene expression level of

these genes in lung metastases to the expression in primary tumors. We did not found significant differential expression between the lung metastases and their primary located tumors by applying both the paired *t* test (DCN, *p* value=0.9; LUM, *p* value=0.5) and the unpaired *t* test (DCN, *p* value=0.9; LUM, *p* value=0.6). Then the expression of both the lung metastases and their primary tumors was compared with the group of non-metastasizing primary cases of GCTB (GCTB-A, GCTB-0, GCTB-R, GCTB-3R, and GCTB-ABC). We observed a significant lower differential gene expression in the lung metastases compared to the non-metastasizing tumor samples (DCN, $p=0.002$; LUM, $p<0.001$). We also found significantly lower expression of both genes in the primary tumors with lung metastases compared to the non-metastasizing tumors (DCN, $p=0.003$; LUM, $p<0.001$) (Fig. 3).

Immunohistochemistry

Immunohistochemical staining for DCN and LUM supported the above findings of lower expression of these proteins in the metastatic GCTB group compared with other groups. Both proteins were mainly present in the extracellular matrix (Fig. 4).

Discussion

GCTB is a heterogeneous tumor with a complex pathobiology. It arises in the epiphysis as an expansile lesion. It has a high recurrence rate and the potential to produce metastatic nodules in the lung; rarely malignant change can also occur in the primary tumor. Morphological features cannot predict GCTB behavior; thus, selected biomarkers could be of value. A few gene expression profiling studies have been carried out on GCTB. Morgan et al. [17] addressed the differential gene expression profiles of neoplastic GCTB mononuclear stromal cells and compared them with those of mesenchymal stem cells. Although many genes were found to be up or downregulated, only gene expression at the cellular level was analyzed. There was no correlation with clinical outcome nor was a search for prognostic biomarkers made. Lee et al. [14] examined the general gene expression profiles of GCTB in relation to other bone tumors, including a number of giant-cell-rich tumors and tumor-like lesions of bone in order to identify novel diagnostic markers. Our study sought to correlate tumor behavior and molecular genetic findings, dividing GCTB into specific clinical subgroups and focusing on gene expression in whole tumor samples, in order to allow us to take the effect of the tumor on the extracellular matrix (ECM) environment and vice versa into account. The ECM is involved in tumor progression and in several crucial biological processes such as cell proliferation, differentiation, adhesion, and migration. In this way, it affects tissue repair and metastatic disease as has frequently been reported for different types of carcinoma [18, 19].

This study has found DCN, LUM, ZNF14, COL11A1, EPYC, and FRZB to be differentially expressed in predefined subgroups of GCTB. Specifically, DCN and LUM showed a lower expression in the metastatic group compared with the non-metastatic group of GCTBs. DCN and LUM are members of the small leucine-rich proteoglycan (SLRP) family: DCN was named for its high affinity interactions with collagen fibers and regulation of fibrillogenesis [20–23]. It has been termed the 'guardian from the matrix' for its presence in the stroma and its multifactorial ways of repressing tumor growth by attenuating key prosurvival, migratory, proliferative, and angiogenic signaling in the tumor microenvironment. DCN has a promiscuous binding capacity and is known to regulate bioavailability of growth factors (e.g., TGF-β) [24–26]. It also acts as an endogenous pan-tyrosine kinase inhibitor, negatively affecting cell proliferation by controlling the endogenous level of modulators of the cell cycle check points [11, 20, 23, 26, 27]. In addition, it influences inflammation and angiogenesis in the tumor microenvironment [23]. LUM has similar functions in the extracellular matrix, however, it has not been studied as extensively [22, 28]. It has been shown that LUM significantly decreases cell migration, invasion, and anchorage-independent growth in vitro [29]. The role of these leucine-rich proteins as tumorigenic inhibitors has been discovered for several epithelial tumors: DCN and LUM were simultaneously found to be less expressed in breast carcinomas and melanomas [22, 30, 31]. Troup et al. [30] reported that decreased expression of DCN and LUM is associated with poorer prognosis in breast carcinoma. A study published by Goldoni et al. [26] showed that in cases of orthotopic breast carcinoma in mice, systemic delivery of DCN reduces pulmonary metastases. In vitro studies have also demonstrated correlation of LUM expression in osteosarcoma cell lines: positively with differentiation and negatively with growth [31]. This study is the first to demonstrate differential expression of SLRPs in whole tumor samples of GCTB exhibiting different biological behavior.

Signaling in GCTB includes attraction of monocytes and induction of osteoclast differentiation and osteoclast activity. The canonical pathway of osteoclast formation, which is well recognized to operate in GCTB, requires the presence of macrophage colony stimulating factor (M-CSF) and the receptor activator for NFκB ligand (RANKL) [32]. There are also non-canonical pathways of osteoclast formation, whereby cytokines or growth factors can substitute for RANKL or M-CSF to induce osteoclast formation. RANKL substitutes include tumor necrosis factor α (TNF-α), transforming growth factor β (TGF-β), interleukin-6 (IL-6), and tumor necrosis factor (ligand) superfamily, member 14 (LIGHT). M-CSF substitutes include vascular endothelial growth factor

Table 2 Most differentially expressed genes in GCTB-M, GCTB-R, GCTB-A, GCTB-ABC, and GCTB-3R, ranked on R value

GCTB subtype	Gene	Accession number NCBI	Average *p* value	Average R value	Fold change	Locus
	Upregulated genes					
Metastatic cases	SLC5A8	NM_145913.3	2.23E-08	2.42	11.25	12q23.1–q23.2
	ERGIC1	NM_020462.1	2.96E-11	1.84	6.3	5q35.1
Relapse cases	ZNF14	NM_021030.2	0.08	1.45	4.26	9p13.3–p13.2
	USP49	NM_018561.3	0.07	1.31	3.71	6p21
	FAM115C	NM_001130026.2	0.06	1.04	2.83	7q35
Aggressive cases	No protein-coding genes					
Regressive cases	EPYC	NM_004950.4	0.009	2.25	9.49	12q21
GCTB with secondary ABC	FGFBP2	NM_031950.3	0.002	2.56	12.94	4p15.32d
	C2orf40	NM_032411.2	0.005	2.23	9.3	2q12.2
	FRZB	NM_001463.3	0.008	1.75	5.75	2q32.1
	Downregulated genes					
Metastatic cases	LUM	NM_002345.3	3.11E-10	−3.41	30.27	12q21.3–q22
	DCN	NM_133503.2	4.38E-08	−3.29	26.85	12q21.33
	OSTC	NM_021227.3	3.15E-08	−2.74	15.49	4q25
	FAM198B	NM_016613.6	2.04E-10	−2.73	15.33	4q32.1
	ITGAV	NM_002210.4	1.66E-09	−2.70	14.88	2q31–q32
	PRDX4	NM_006406.1	4.58E-10	−2.56	12.94	Xp22.11
	TMCO3	NM_017905.4	2.22E-09	−2.26	9.58	13q34
	RPL9	NM_001024921.2	4.67E-09	−2.19	8.94	4p13
	EIF3M	NM_006360.4	3.81E-10	−2.15	8.58	11p13
	KDELR2	NM_006854.3	2.15E-10	−2.11	8.2	7p22.1
	MMADHC	NM_015702.2	1.25E-09	−1.94	6.96	2q23.2
Relapse cases	DPT	NM_001937.4	0.06	−1.73	5.64	1q12–q23
Aggressive cases	COL11A1	NM_080629.2	0.01	−1.62	4.9	1p21
Regressive cases	RPL23	NM_000978.3	0.07	−1.53	4.62	17q
	CLEC2D	NM_013269.5	0.04	−1.39	4.01	12p13
GCTB with secondary ABC	No protein-coding genes					

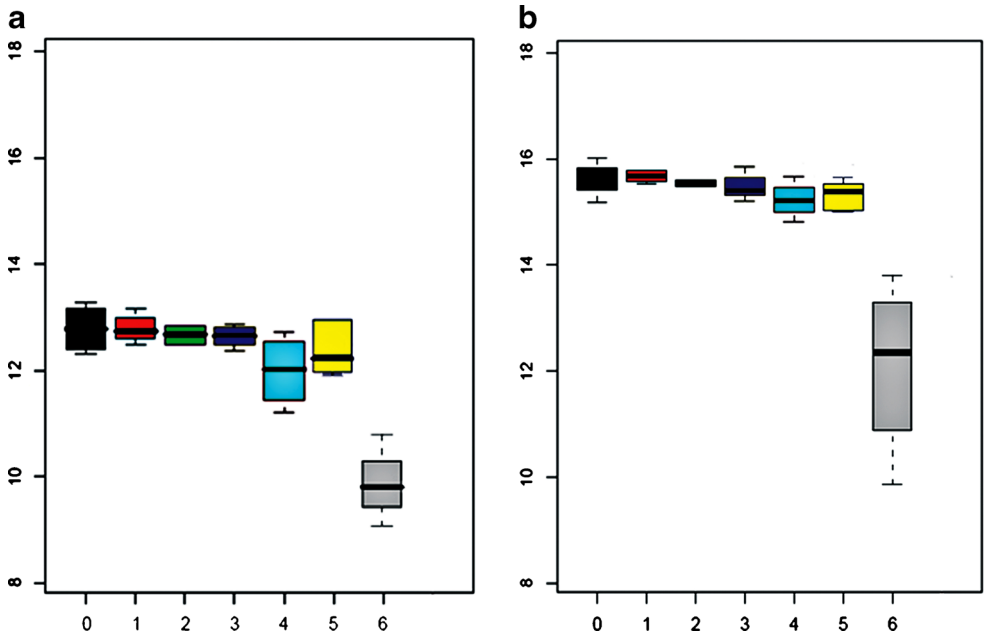

Fig. 1 Boxplot for LUM (**a**) and DCN (**b**). *Y*-axis, $\log^2$-transformed normalized microarray data. *X*-axis, GCTB group. *0* GCTB-O, *1* GCTB-R, *2* GCTB-3R, *3* GCTB-A, *4* GCTB-ABC, *5* ABC, *6* GCTB-M

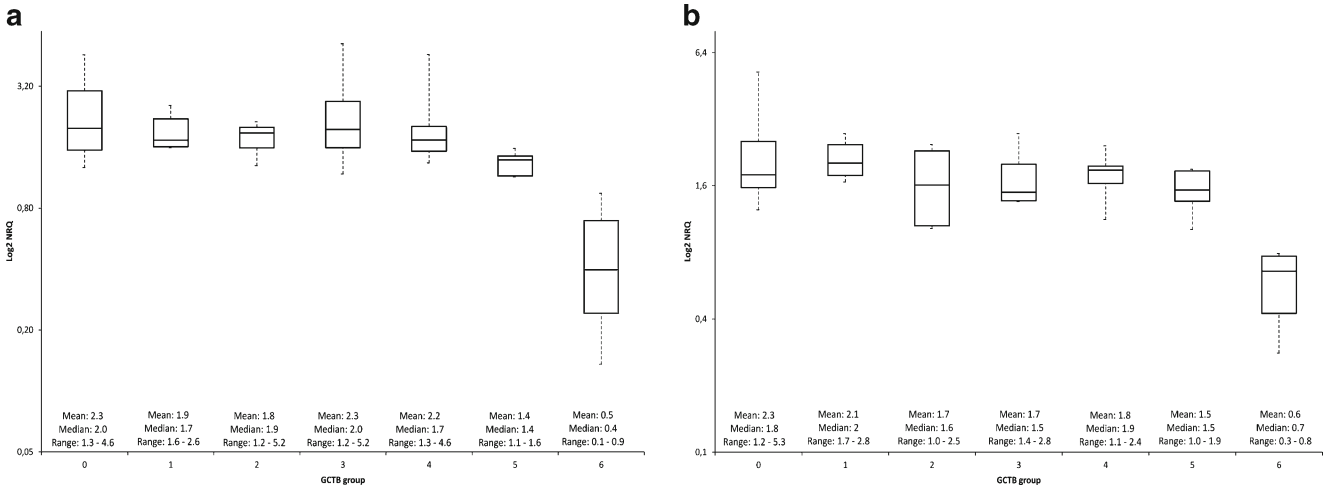

Fig. 2 Boxplot for Q-PCR values of LUM (**a**) and DCN (**b**) expression. *Y*-axis, $\log^2$-transformed normalized relative quantity (NRQ) including mean, median, and range of expression. *X*-axis, GCTB group. *0* GCTB-O, *1* GCTB-R, *2* GCTB-3R, *3* GCTB-A, *4* GCTB-ABC, *5* ABC, *6* GCTB-M

(VEGF), placental growth factor (PlGF), Fms-like tyrosine kinase 3 (FLT-3) ligand, and hepatocyte growth factor (HGF). These growth factors can also influence canonical (RANKL/M-CSF-induced) osteoclast formation [32–34]. Addition of TGF-β to RANKL and M-CSF increases osteoclast formation, whereas blocking endogenous TGF-β significantly inhibits osteoclast formation [35]. We found lower expression of DCN and LUM in metastasizing GCTB, which is plausible because of the known functions of DCN: the mechanisms of DCN inhibition in GCTB include sequestration of TGF-β, which would reduce monocyte attraction and osteoclast differentiation and osteoclast activity, blocking of tyrosine kinase receptors (TKR), such as HGF receptor (MET) and VEGF receptor (VEGFR), which would reduce angiogenesis and osteoclast activity through repression of β-catenin and hypoxia-inducible factor 1-alpha (HIF-1α) and attenuation of matrix metalloprotein 9 (MMP-9) [23, 32, 36–38]. The M-CSF receptor is also a TKR, but there is no evidence of direct inhibition of monocytes by DCN in the literature. A reduction in DCN would then imply less attenuation of osteoclast-ECM signaling, possibly enhancing the production of lung implants. Changes in DCN have variable effects in different neoplastic or reactive conditions [23] and the effect of DCN signaling inhibition needs validation in GCTB.

LUM's mechanism in GCTB remains unclear; LUM and DCN are situated next to each other on the long arm of chromosome 12. This strongly suggests a possible coordination of transcriptional or post-transcriptional control over these SLRPs. LUM may be an innocent bystander, or it may have important, hitherto unknown functions.

Differential gene expression between primary GCTB and lung metastasis may be expected. We, therefore, investigated

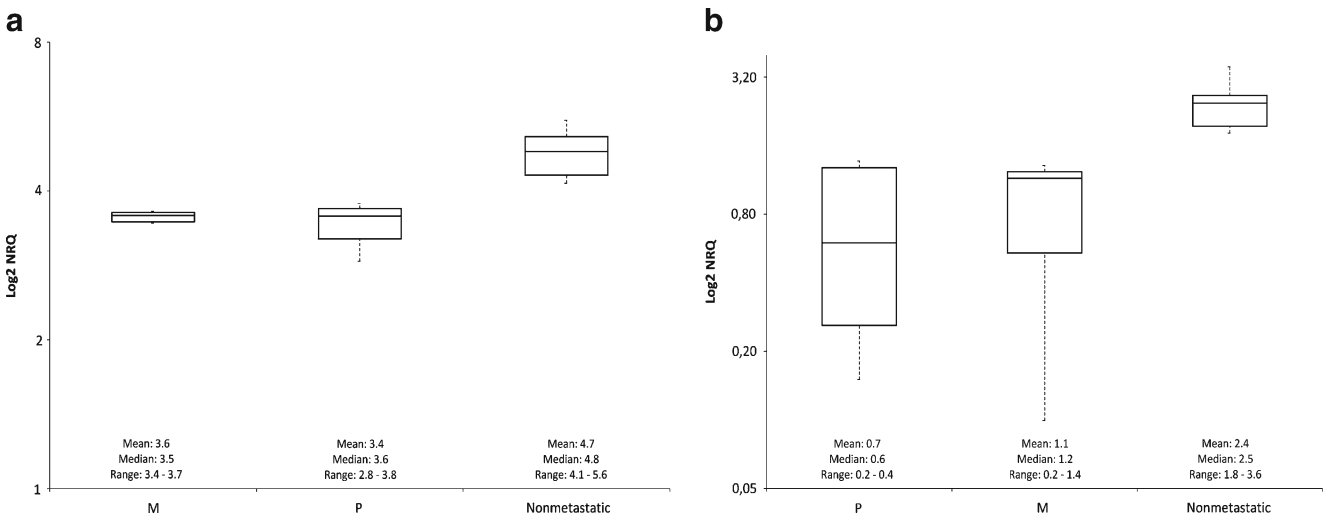

Fig. 3 Boxplot for LUM (**a**) and DCN (**b**) expression in lung metastases (M), their primary tumor (P) and non-metastasizing tumor samples (Non metastatic). *Y*-axis, $\log^2$-transformed NRQ including mean, median, and range of expression. *X*-axis, GCTB group. *0* GCTB-O, *1* GCTB-R, *2* GCTB-3R, *3* GCTB-A, *4* GCTB-ABC, *5* ABC, *6* GCTB-M

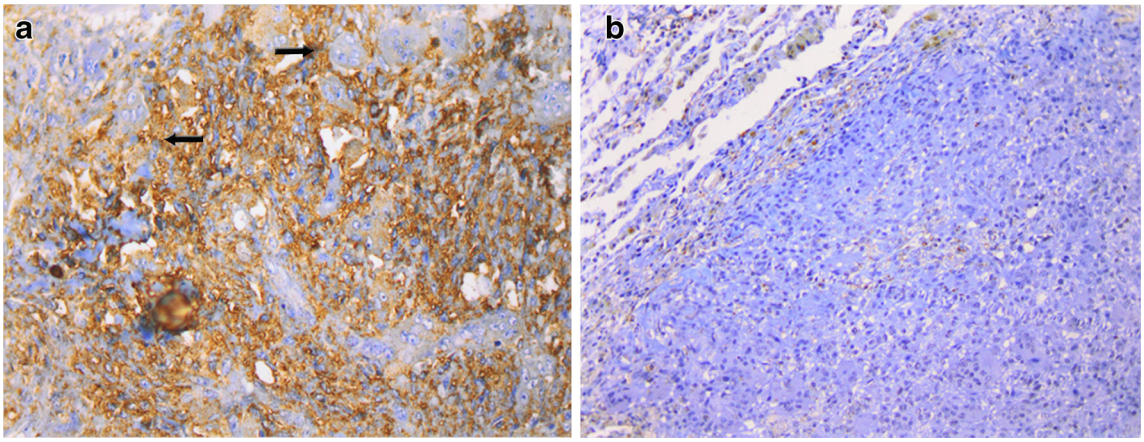

Fig. 4 Immunostaining for DCN. A clear stronger protein expression was found in the control group (patient 3) (**a**) compared with lung metastatic nodules of GCTB (patient 44) (**b**)

whether lower expression of these extracellular matrix proteins is a tumor specific rather than a location specific phenomenon. Expression of both extracellular matrix genes, which differs significantly between metastasizing and non-metastasizing tumors and between primary tumors compared to the non-metastasizing group, is a strong indication that the expression of LUM and DCN is tumor specific. Lower differential gene expression of these ECM genes is a potential biomarker for their biological behavior. However, it is not clear whether these markers can be used in routine pathology, since quantitative immunohistochemistry might have low reproducibility.

In comparing recurrent and non-recurrent GCTBs, this study found that DPT is less expressed in the recurrent group. DPT encodes another protein related to the ECM. Reduced DPT has previously been detected in some leiomyomas, and involvement in progression of these tumors has been suggested. Examination of the extracellular matrix in these leiomyomas revealed disorganized matrix microenvironment that could favor tumor growth [39]. Other studies have reported that DPT interacts with collagen in the ECM, modulating its structure [40]. DPT, DCN, and TGF-β display complex interactions, the effects of which have yet to be elucidated [41]. In addition to DPT, zinc finger protein 14 (ZNF14) also exhibited differential mRNA expression in the recurrent cases compared with the other groups. ZNF14 is known to bind a number of zinc finger proteins, repressing their transcription [42]. Repression of tumor suppression genes associated with increased ZNF14 may promote tumor progression and recurrence; this may explain the elevated transcription levels in the recurrent cases of GCTB as noted in this study.

GCTBs in the radius, which are known to exhibit more aggressive behavior, showed differential expression of COL11A1. COL11A1 encodes one of the two alpha chains of type XI collagen, a fibrillar collagen in the ECM which plays an important role during fibrillogenesis. Low COL11A1 expression level may lead to decreased synthesis of collagen type XI and thus to a reduction in this type of collagen fibrils, causing a less solid or less uniform ECM structure [43]. Thus, weakening of ECM in these tumors might co-contribute to their aggressiveness.

In contrast, tumors which show regressive morphological changes showed higher expression of EPYC than those which showed no evidence of regression. Like DCN and LUM, the encoding protein of EPYC is a member of the small leucine-rich proteoglycan family and is located in the ECM [44]. It is involved in chondrogenesis and regulates fibrillogenesis by interacting with collagen fibrils and other extracellular matrix proteins [45]. Based on our research, it is possible that EPYC, DPT, and COL11A1 might (as has been shown for DCN) have an important signaling function on the top of their function in ECM organization.

In the GCTB group associated with ABC, FRZB was differentially upregulated: It functions as a soluble decoy receptor for Wnt signaling and exerts a positive effect on osteoblast differentiation, possibly explaining the ABC subtype [46].

In conclusion, we have shown that DCN, LUM, DPT, ZNF14, COL11A1, EPYC, and FRZB represent promising molecular markers to study tumor biology in GCTB with respect to metastatic potential, tumor recurrence, local aggressiveness, regressive changes, and secondary ABC change. Strongly reduced expression of DCN and LUM in lung metastases and their corresponding primary tumors emphasizes their importance in the biological behavior of GCTB.

Acknowledgments This study was partially carried out by the EuroBoNet Consortium, a Network of Excellence funded by the EU.

Contributions of authors M Lieveld designed the research study, performed Q-PCR research, interpreted the data, and wrote the paper

E Bodson contributed to writing of the paper and interpretation of the data

G De Boeck performed research (microarray)

B Nouman: contribution of samples and performed research (Q-PCR)

AM Cleton-Jansen performed research (microarray)
E Korsching analyzed the microarray data
MS Benassi and P Picci: contribution of samples
G Sys and B Poffyn: contribution of samples
NA Athanasou: revision and final approval of the article
PCW Hogendoorn: contribution of samples and examination of samples
RG Forsyth designed the research study and examined samples

Manufacturer's name Illumina's Human-6 v2 Expression BeadChips (Illumina®, Son, The Netherlands)
Trizol® (Invitrogen Life Technologies, Carlsbad, CA)
RNeasy-mini kit (Qiagen, Hilden, Germany)
NanoDrop ND-100 Spectrophotometer (Nanodrop® Technologies Inc., Wilmington, DE)
Agilent 2100 Bioanalyzer (Agilent Technologies, Palo Alto, CA)
Illumina® TotalPrep RNA Amplification Kit (Ambrion, Inc., Austin, TX)
RQ1 RNase–Free DNase (Promega, Leiden, The Netherlands)
iScript cDNA synthesis kit (Biorad Laboratories Ltd. Hertfordshire, UK)
GeNorm Housekeeping Gene Selection Kit (Primerdesign, Southampton, Hants)
Lightcycler® 480 (Roche Diagnostics, Vilvoorde, Belgium)
Sybr Green mix (Roche Diagnostics, Vilvoorde, Belgium)
Antibodies (Abcam, UK)
Electrically charged superfrost plus slides (Menzel-Gläser, Braunschweig)
Peroxidase DAB (DAKO, Heverlee, Belgium)
Streptavidin-HRP (DAKO, Heverlee, Belgium)

Conflict of interest All authors state that they have no conflicts of interest.

References

1. Zheng MH, Fan Y, Wysocki SJ et al (1994) Gene expression of transforming growth factor-beta 1 and its type II receptor in giant cell tumors of bone. Possible involvement in osteoclast-like cell migration. Am J Pathol 145(5):1095–1104
2. Joyner CJ, Quinn JM, Triffitt JT, Owen ME, Athanasou NA (1992) Phenotypic characterisation of mononuclear and multinucleated cells of giant cell tumour of bone. Bone Miner 16(1):37–48
3. Lindeman JH, Hanemaaijer R, Mulder A et al (2009) Cathepsin K is the principal protease in giant cell tumor of bone. Am J Pathol 165: 593–600
4. Forsyth RG, De Boeck G, Taminiau AHM et al (2009) CD33+ CD14 − phenotype is characteristic of multinuclear osteoclast-like cells in giant cell tumor of bone. J Bone Miner Res 24(1):70–77
5. da Costa CET, Annels NE, Faaij CMJM, Forsyth RG, Hogendoorn PCW, Egeler RM (2005) Presence of osteoclast-like multinucleated giant cells in the bone and nonostotic lesions of Langerhans cell histiocytosis. J Exp Med 201(5):687–693
6. Reid R, Banerjee SS, Sciot R (2002) WHO classification of tumors of bone: giant cell tumor. In: world health organization classification of tumors. Pathology and genetics of tumors of soft tissue and bone. IARC Press, Lyon, pp 310–312
7. Edwards JR, Williams K, Kindblom LG et al (2008) Lymphatics and bone. Hum Pathol 39:49–55
8. Blackley HR, Wunder JS, Davis AM, White LM, Kandel R, Bell RS (1999) Treatment of giant cell tumors of long bones with curettage and bone grafting. J Bone Joint Surg 81:811–820
9. Turcotte RE (2006) Giant cell tumor of bone. Orthop Clin North Am 37:35–51
10. Marcove RC, Sheth DS, Brien EW, Huvos AG, Healey JH (1994) Conservative surgery for giant cell tumors of sacrum. The role of cryosurgery as a supplement to curettage and partial excision. Cancer 74:1253–1260
11. Domovitov SV, Healey JH (2010) Primary malignant giant-cell tumor of bone has high survival rate. Ann Surg Oncol 17:694–701
12. Balke M, Schremper L, Gebert C et al (2008) Giant cell tumor of bone: Treatment and outcome of 214 cases. J Cancer Res Clin Oncol 134:969–978
13. Bertoni F, Bacchini P, Staals E (2003) Malignancy in giant cell tumor of bone. Cancer 97:2520–2529
14. Lee C, Espinosa I, Jensen KC et al (2008) Gene expression profiling identifies p63 as a diagnostic marker for giant cell tumor of bone. Mod Pathol 21:531–539
15. Moskovszky L, Dezsö K, Athanasou NA et al (2010) Centrosome abnormalities in giant cell tumor of bone: Possible association with chromosomal instability. Mod Pathol 23:359–366
16. Moerkerke B, Goetghebeur E (2006) Selecting "significant" differentially expressed genes from the combined perspective of the null and the alternative. J Comput Biol 13:1513–1531
17. Morgan T, Atkins GJ, Trivett MK et al (2005) Molecular profiling of giant cell tumor of bone and the osteclastic localization of ligand for receptor activator of nuclear factor κ B. Am J Pathol 167:117–128
18. Hocking AM, Shinomura T, McQuillan DJ (1998) Leucine-rich repeat glycoproteins of the extracellular matrix. Matrix Biol 17:1–19
19. Pupa SM, Ménard S, Forti S, Tagliabe E (2002) New insights into the role of extracellular matrix during tumor onset and progression. J Cell Physiol 192:259–267
20. Schaefer L, Iozzo RV (2008) Biological functions of the small leucine-rich proteoglycans: from genetics to signal transduction. J Biol Chem 31:21305–21309
21. Danielson KG, Baribault H, Holmes DF, Graham H, Kadler KE, Iozzo RV (1997) Targeted disruption of decorin leads to abnormal collagen fibril morphology and skin fragility. J Cell Biol 136:729–743
22. Chakravarti S, Magnuson T, Lass JH, Jepsen KJ, LaMantia C, Carroll H (1998) Lumican regulates collagen fibril assembly: Skin fragility and corneal opacity in the absence of lumican. J Cell Biol 141:1277–1286
23. Neill T, Schaefer L, Iozzo RV (2012) Decorin: a guardian from the matrix. Am J Pathol 181(2):380–387
24. Kaname S, Ruoslahti E (1996) Betaglycan has multiple binding sites for transforming growth factor-beta 1. Biochem J 315:815–820
25. Cabello-Verrugio C, Brandan E (2007) A novel modulatory mechanism of transforming growth factor-β signaling through decorin and LRP-1. J Biol Chem 282:18842–18850
26. Goldoni S, Humphries A, Nyström A et al (2009) Decorin is a novel antagonistic ligand of the Met receptor. J Cell Biol 185:743–754
27. Zhu JX, Goldoni S, Bix G et al (2005) Decorin evokes protracted internalization and degradation of the epidermal growth factor receptor via caveolar endocytosis. J Biol Chem 280:32468–32479
28. Nikitovic D, Katonis P, Tsatsakis A, Karamanos NK, Tzanakakis GN (2008) Lumican, a small leucine-rich proteoglycan. IUBMB Life 60(12):818–823
29. Vuillermoz B, Khoruzhenko A, D'Onofrio MF et al (2004) The small leucine-rich proteoglycan lumican inhibits melanoma progression. Exp Cell Res 296:294–306
30. Troup S, Njue C, Kliewer EV et al (2003) Reduced expression of the small leucine-rich proteoglycans, lumican, and decorin is associated with poor outcome in node-negative invasive breast cancer. Clin Cancer Res 9:207–214
31. Nikitovic D, Berdiaki A, Zafiropoulos A et al (2008) Lumican expression is positively correlated with the differentiation and

negatively with the growth of human osteosarcoma cells. FEBS J 275(2):350–361
32. Knowles HJ, Athanasou NA (2009) Canonical and non-canonical pathways of osteoclast formation. Histol Histopathol 24(3):337–346
33. Wallenius V, Hisaoka M, Helou K et al (2000) Overexpression of the hepatocyte growth factor (HGF) receptor (Met) and presence of a truncated and activated intracellular HGF receptor fragment in locally aggressive/malignant human musculoskeletal tumors. Am J Pathol 156(3):821–829
34. Taylor RM, Kashima TG, Knowles HJ, Athanasou NA (2012) VEGF, FLT3 ligand, PlGF and HGF can substitute for M-CSF to induce human osteoclast formation: implications for giant cell tumour pathobiology. Lab Invest 92(10):1398–1406
35. Itonaga I, Sabokbar A, Sun SG, Kudo O, Danks L, Ferguson D, Fujikawa Y, Athanasou NA (2004) Transforming growth factor-beta induces osteoclast formation in the absence of RANKL. Bone 34(1): 57–64
36. Kumta SM, Huang L, Cheng YY, Chow LT, Lee KM, Zheng MH (2003) Expression of VEGF and MMP-9 in giant cell tumor of bone and other osteolytic lesions. Life Sci 73(11):1427–1436
37. Knowles HJ, Athanasou NA (2008) Hypoxia-inducible factor is expressed in giant cell tumour of bone and mediates paracrine effects of hypoxia on monocyte-osteoclast differentiation via induction of VEGF. J Pathol 215(1):56–66
38. Neill E (2012) T, Painter H, Buraschi S et al. Decorin antagonizes the angiogenic network: concurrent inhibition of Met, hypoxia inducible factor 1α, vascular endothelial growth factor A, and induction of thrombospondin-1 and TIMP3. J Biol Chem 287(8):5492–5506
39. Catherino WH, Leppert PC, Stenmark MH et al (2004) Reduced dermatopontin expression is a molecular link between uterine leiomyomas and keloids. Genes Chromosomes Cancer 40:204–217
40. Okamoto O, Fujiwara S, Abe M, Sato Y (1999) Dermatopontin interacts with transforming growth factor β and enhances its biological activity. Biochem J 337:537–541
41. Okamoto O, Fujiwara S (2006) Dermatopontin, a novel player in the biology of the extracellular matrix. Connect Tissue Res 47(4):177–189
42. Groner AC, Meylan S, Ciuffi A et al (2010) KRAB-zinc finger proteins and KAP1 can mediate long-range transcriptional repression through heterochromatin spreading. PLoS Genet 6:e1000869
43. Robin NH, Moran RT, Warman M, Ala-Kokko L. Stickler Syndrome. GeneReviews. http://www.ncbi.nlm.nih.gov/books/NBK1302/. Accessed Nov 3 2011
44. Johnson HJ, Rosenberg L, Choi HU, Garza S, Höök M, Neame PJ (1997) Characterization of epiphycan, a small proteoglycan with a leucine-rich repeat core protein. J Biol Chem 272:18709–18717
45. Knudson CB, Knudson W (2001) Cartilage proteoglycans. Semin Cell Dev Biol 12:69–78
46. Chung YS, Baylink DJ, Srivastava AK et al (2004) Effects of secreted frizzled-related protein 3 on osteoblasts in vitro. J Bone Miner Res 19(9):1395–1402